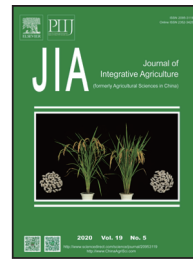




Available online at www.sciencedirect.com

ScienceDirect



RESEARCH ARTICLE

Using an image segmentation and support vector machine method for identifying two locust species and instars



Shuhan LU¹, YE Si-jing^{2, 3}

¹ Department of Computer and Information Science, College of Art and Science, Ohio State University, Columbus, OH 43210, USA

² State Key Laboratory of Earth Surface Processes and Resource Ecology, Beijing Normal University, Beijing 100875, P.R.China

³ Center for Geodata and Analysis, Beijing Normal University, Beijing 100875, P.R.China

Abstract

Locusts are agricultural pests around the world. To cognize how locust distribution density and community structure are related to the hydrothermal and vegetation growth conditions of their habitats and thereby providing rapid and accurate warning of locust invasions, it is important to develop efficient and accurate techniques for acquiring locust information. In this paper, by analyzing the differences between the morphological features of *Locusta migratoria manilensis* and *Oedaleus decorus asiaticus*, we proposed a semi-automatic locust species and instar information detection model based on locust image segmentation, locust feature variable extraction and support vector machine (SVM) classification. And we subsequently examined its applicability and accuracy based on sample image data acquired in the field. Locust image segmentation experiment showed that the proposed GrabCut-based interactive segmentation method can be used to rapidly extract images of various locust body parts and exhibits excellent operability. In a locust feature variable extraction experiment, the textural, color and morphological features of various locust body parts were calculated. Based on the results, eight feature variables were selected to identify locust species and instars using outlier detection, variable function calculation and principal component analysis. An SVM-based locust classification experiment achieved a semi-automatic detection accuracy of 96.16% when a polynomial kernel function with a penalty factor parameter c of 2040 and a gamma parameter g of 0.5 was used. The proposed detection model exhibits advantages such as high applicability and accuracy when it is used to identify locust instars of *L. migratoria manilensis* and *O. decorus asiaticus*, and it can also be used to identify other species of locusts.

Keywords: locust identification, machine learning, support vector machine, *L. migratoria manilensis*, *O. decorus asiaticus*

1. Introduction

Received 24 June, 2019 Accepted 22 November, 2019
Correspondence YE Si-jing, Mobile: +86-13488811751, E-mail: yesj@bnu.edu.cn

© 2020 CAAS. Published by Elsevier Ltd. This is an open access article under the CC BY-NC-ND license (<http://creativecommons.org/licenses/by-nc-nd/4.0/>).
doi: 10.1016/S2095-3119(19)62865-0

Locusts are agricultural pests around the world (Ren *et al.* 2017). Globally, an area of nearly 50 million ha is infested by locusts each year, and approximately 1/8 of the world's population is affected by locust invasions (Wang *et al.* 2017). Since ancient times, China has suffered from frequent locust invasions, where the extent and severity have been the highest in the world. *Locusta migratoria manilensis*, which

causes the most severe damage, is a migratory species that appears suddenly (Din et al. 1978). Therefore, the ability to rapidly and accurately acquire information about the growth conditions, distribution densities (Van der Werf et al. 2005) and community features of locusts (Bryceson et al. 1986; Gómez et al. 2019) is important for the timely and effective prevention and control of locust invasions.

Conventional locust monitoring relies on manual field acquisition of locust species, instar and population data by plant protection specialists. This method has numerous shortcomings, including a high cost of information acquisition, low efficiency, limited coverage, an inability to monitor certain locust-infested areas in the field (e.g., lakes, wetlands and tidal flats), difficulty in identification of species and instars, and proneness to identification errors due to the numerous locust species and morphologies and the complexity of their habitats (Ye et al. 2014). Additionally, since locusts are fast and migratory, manual surveys are unable to respond to rapid changes of the locust distribution density and community features due to their poor time effectiveness.

In recent years, computer vision technologies have undergone rapid development and have been extensively applied in the monitoring and identification of insects (Zhang et al. 2009; Wang 2017; Yao et al. 2017; Deng 2018). At present, there are two main directions in pest identification research at home and abroad: (1) Pest feature is extracted based on computer vision. The recognition methods mostly adopt the global features of pest images, such as color features, morphological features, texture features, etc. Due to the limitation of global feature description, many feature expressions combining local features and global features have emerged in recent years. By improving the image identification rate through the integration of the scale-invariant feature transform (SIFT) and the loss algorithm, various pests including *Diabrotica* (Coleoptera: Chrysomelidae), *Aphis gossypii* Genn., *Thrips tabaci* L. and *Bemisia tabaci* Genn., were identified with high accuracy (Solis-Sánchez et al. 2011). Cai and He (2010) proposed a reverse identification method for identifying pests based on pest-eaten leaves, extracted eigenvalues and constructed a BP neural network identification model; additionally, Cai and He (2010) demonstrated that the proposed method outperformed previous methods in terms of identification efficiency and accuracy. Zhen et al. (2010) identified locusts and calculated population densities by dynamically extracting color, area and morphological features using an image processing technique. Zhang (2013) proposed a maximum-similarity region-merging algorithm combined with texture and color histograms and used it to segment pest images; the results showed that this algorithm was able to satisfactorily extract target pests against a complex farmland

background. Zhang (2013) also proposed a crop pest image identification method based on multifeature fusion and demonstrated its high accuracy through experiments. A locust identification model was proposed based on near-infrared spectroscopy and hierarchical clustering, Xiong et al. (2007) examined the feasibility of the model for rapidly detecting locusts in complex environments with interlaced vegetation, soil and rocks, and found that it achieved an accuracy up to 91.67%. (2) Classification models were selected and optimized based on machine learning. The main classifiers used were support vector machine (SVM) classifier, neural network, K-nearest neighbor, principal component analysis and so on. Compared with traditional methods, deep learning model could self-learn the relationship, which is expressed by directly-driven data sets. An intelligent identification system was constructed in process of feature automatic learning, feature fausion, classification and position regression calculation framework of pest species based on deep learning method, the recognition rates of 16 kinds of common pests in light traps under natural condition ranged from 66 to 90% (Chen et al. 2019). Thenmozhi and Srinivasulu (2019) proposed an efficient convolutional neural network (CNN) model to classify insect species' datasets which have relatively high efficiency. Transfer learning was applied to fine tune the pre-trained models. The data augmentation techniques such as reflection, scaling, rotation, and translation are also applied to prevent the network from overfitting. The effectiveness of hyperparameters was analyzed in the proposed model to improve accuracy. The highest classification accuracy of 96.75, 97.47, and 95.97% was achieved in proposed CNN model for the National Bureau of Agricultural Insect Resources (NBAIR) insect dataset (40 classes), Xie1 insect dataset (24 classes) (Xie et al. 2015) and Xie2 insect dataset (40 classes) (Xie et al. 2018), respectively. Many deep learning networks have been successfully applied to target detection, such as faster region-CNN (R-CNN), single shot multibox detector (SSD), RetinaNet and so on. However, the models were designed for pattern analysis statistical modeling and computational learning volatile organic compounds (PASCAL VOC), Microsoft common objects in context (COCO) and other universal large data sets. The intraclass variation of the target was small and the interclass variation was large.

In this paper, we proposed a semi-automatic locust species and instar information detection model based on locust image segmentation, locust feature variable extraction and SVM classification and subsequently examined its applicability and accuracy based on sample image data for locust instars of *L. migratoria manilensis* and *Oedaleus decorus asiaticus* (including locusts of the 4th-instar, 5th-instar and adult stages) collected in the

field. The achievement of this paper will be helpful to the generalization of deep learning model.

2. Materials and methods

2.1. Experimental data

SVM-based locust species and instar identification often requires the support of training samples to improve the reliability and robustness of the classification model. In this study, a visible light camera was used to acquire image data for locust instars of the species *L. migratoria manilensis* and *O. decorus asiaticus* (including 4th-instar, 5th-instar and adult locusts of both species) in complex field environments. The *L. migratoria manilensis* data were acquired in a plant protective station in the Dagang District of Tianjin, and the *O. decorus asiaticus* data were acquired in a wheat field in Ar Horqin Banner in the Chifeng City, Inner Mongolia, China. During the data acquisition process, we used macro lens to capture images of locusts of the species *L. migratoria manilensis* and *O. decorus asiaticus* in various states (including sideways, recumbent, upright and partially occluded) at close distances and various view angles (including side and top views). In addition, we used a wide-angle lens to photograph multiple locusts in one frame from a distance of 1–2 m in the front- and top-view directions, as shown in Fig. 1. The acquired images were categorized into six groups based on the locust instar and species. Subsequently, 200 sample images that met the specified criteria in terms of image sharpness and diversity of perspectives, target states and photographic scales were selected from each group. Thus, a dataset of 1200 sample

images was constructed. Six data sets were designed. The data sets of group A included 4th-instar age, 5th-instar age and adult of *L. migratoria manilensis*, 100 locust images were trained and 100 locusts were tested. The data sets of *O. decorus asiaticus* were the same as above, which was group B.

2.2. Analysis of the morphological features of locusts

The locust is an insect of the order Orthoptera and has two main growth stages, namely, nymph and adult. The nymph stage can generally be further divided into several substages, such as the first, second, third, fourth and fifth instars. The objective of this study was to achieve semi-automatic identification of locust instars of the species *L. migratoria manilensis* and *O. decorus asiaticus*. The study objects have the same body shape but differ significantly in external morphology (Guo et al. 2004; Lu et al. 2006; Wen et al. 2015). The external morphological characteristics of the two locust species are shown in Table 1.

2.3. Locust image segmentation methods

Graph-theory-based segmentation methods mainly include the GrabCut and GraphCut techniques. GrabCut is an improved graph cut method in which a vector $Z=\{Z_1, Z_2, Z_3, \dots, Z_n, \dots, Z_N\}$ is used to represent an image and the image segmentation process is transformed into the calculation of a value for each pixel, denoted by $\alpha=\{\alpha_1, \alpha_2, \dots, \alpha_n, \dots, \alpha_N\}$, $\alpha_n \in \{0, 1\}$ (for a pixel α_n , if its value is 0, it belongs to the background; if its value is 1, it belongs to the foreground) (Wang et al. 2014). The GrabCut method uses two Gaussian

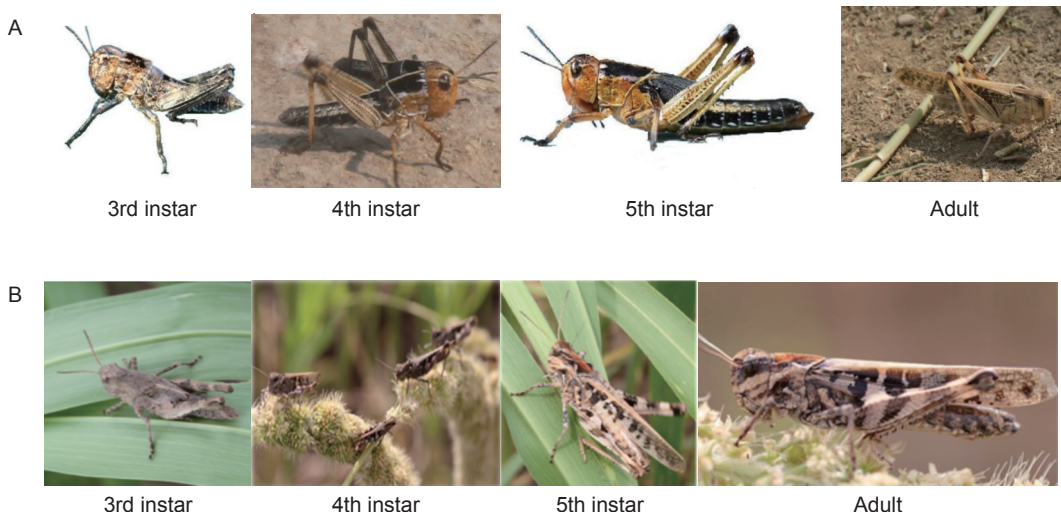


Fig. 1 Locust samples collected in the field. A, sample images of *Locusta migratoria manilensis*. B, sample images of *Oedaleus decorus asiaticus*.

Table 1 Comparison of the external morphologies of locust instars of *Locusta migratoria manilensis* and *Oedaleus decorus asiaticus*

Species	Instar	Number of antennal segments	Pronotum	Wing buds	Body length (mm)	Body color
<i>L. migratoria manilensis</i>	1st	13–14	The posterior margin of the pronotum is relatively flat and straight.	Inconspicuous	5–10	Black
	2nd	18–19	The pronotum extends backward, and the middle of its posterior margin protrudes slightly backward.	There is no significant difference between the forewing and hind wing buds, and the apices of the wings point downward.	8–14	Black (body) and reddish-brown (head)
	3rd	20–21	The anterior margin of the pronotum extends forward, and its posterior margin notably extends backward, covers the mesothorax and exhibits an obtuse angle.	The wind buds are conspicuous. The forewing buds are notably smaller than the hind wing buds. The hind wing buds have a slightly triangular shape. The apices of the wings point backward.	10–20	Black (body) and reddish-brown (head)
	4th	22–23	The posterior margin of the pronotum extends further backward and covers the back of the mesothorax and metathorax, and its angle decreases.	The wing buds extend to approximately the second segment of the abdomen and are close to the back. The apices of the wings point backward.	16–25	Blackish-brown (back of the body), light yellow (hind tibiae) and reddish-brown (head)
	5th	24–25	The posterior margin of the pronotum extends backward and covers the back of the mesothorax and metathorax.	The wing buds extend to the fourth and fifth segments of the abdomen. The forewing buds are narrow and long, are covered by the hind wing buds and fold towards the back. The apices of the wings point backward.	26–40	Blackish-brown (back of the body), light yellow (hind tibiae) and reddish-brown (head)
	Adult	–	–	The ratio of the forewing length to the hind femur length is greater than 2.	33–52	Blackish-brown (back of the body), light yellow (hind tibiae) and reddish-brown (head)
<i>O. decorus asiaticus</i>	1st	13	The anterior thoracic plate has a deep ridged back ridge	Unexplained big and hypertrophic	4.79–6.85	black
	2nd	17	The anterior thoracic plate is ridged-like, the center of the leading edge protrudes forward and the tip is slightly concave.	Significantly extend the edge of the back plate	7.03–10.78	First six sections are black brown, color gradually becomes lighter, the end is yellowish brown
	3rd	20–21	The center of the leading edge is slightly pointed, the center of the trailing edge is slightly concave, and the entire trailing edge is curved.	Males' wing buds are on the back, growing to the trailing edge of the first abdominal segment. The hind wings are significantly longer than the fore wings. Females' are significantly wider back side of the back side, with fore wing oval and hind wing heart shape.	9.04–14.3	End color dark
	4–5th	23	The center of the leading edge is slightly pointed, the trailing edge is female, and the male is obtuse.	Male wing buds reach the trailing edge of the third abdominal segment. The female turns to the back and reaches the trailing edge of the first abdominal section.	13.28–19.44	End color dark
	Adult	24	The center of the leading edge is slightly pointed and pointed, and the trailing edge is obtuse	The wing bud grows to the rear of the third abdominal segment or the middle of the fourth abdominal segment. The hind wing is slightly longer than the fore wing, and the wing tip points to the rear.	18.36–30.27	The end is black and is becoming lighter to the fore side

mixture models (GMMs), one for the background and one for the foreground. Each GMM is composed of a mixture of K Gaussian models (generally, $K=5$). Each pixel has a parameter k_n ($k_n \in \{1, \dots, K\}$). Whether the parameter comes from the background or the foreground depends on the value of α_n . Eq. (1) shows the Gibbs energy function calculation process for the GrabCut method. In eq. (1), $\mu(\cdot)$ is the Gaussian probability distribution, $\pi(\cdot)$ is a mixed weight coefficient, the parameter θ can be represented as shown in eq. (2), and the smoothing term V is calculated using the euclidean distance in the Red Green Blue (RGB) space (eq. (3)). $p(\cdot)$ represents Gaussian introduction distribution and $\pi(\cdot)$ represents mixed weight coefficient.

$$E(a, k, \theta, z) = \sum_n D(a_n, k_n, \theta, z_n) + V(a, z) \quad (1)$$

U is defined as:

$$U(a, k, \theta, z) = \sum_n D(a_n, k_n, \theta, z_n) \quad (2)$$

D is defined as:

$$D(a_n, k_n, \theta, z_n) = -\log p(z_n | a_n, k_n, \theta) - \log \pi(a_n, k_n) \quad (3)$$

$$D(a_n, k_n, \theta, z_n) = -\log \pi(a_n, k_n) + 0.5 \log \det \Sigma(a_n, k_n) + 0.5 [z_n - \mu(a_n, k_n)]^T \Sigma(a_n, k_n)^{-1} [z_n - \mu(a_n, k_n)] \quad (4)$$

$$\theta = \{\pi(a, k), \mu(a, k), (a_n, k_n), a=0, 1, k=1, \dots, K\} \quad (5)$$

$$V(a, z) = \gamma \sum_{(m, n) \in C} [\alpha_n \neq \alpha_m] \exp -\beta \|z_m - z_n\|^2 \quad (6)$$

The GrabCut method was employed to separate and extract various target body parts (i.e., the head, wings, pronotum and hind legs) from locust images with complex backgrounds. First, we acquired locust images in an indoor environment and performed GrabCut-based automatic segmentation of the body parts. Due to the significant differences between the foregrounds and backgrounds in the images, excellent segmentation results were obtained. However, because of the complexity of the field environments, the results obtained from automatic segmentation performed directly on field images using the GrabCut method were unstable and contained relatively

large errors, as shown in Fig. 2. In view of this problem, we employed an interactive automatic-manual labeling method to segment the images. The background and foreground contours with relatively large errors in the images, which were semi-automatically segmented based on GrabCut, were manually labeled, and the GrabCut method was then used again to correct the segmented images.

The steps of the interactive segmentation process are as follows:

Step 1: Initialization

1.1) Construct a rectangular frame to label the target object and initialize the sample image T by the following: setting the pixels outside the rectangular frame as belonging to the image background region T_B (trimap background), the pixels within the rectangular frame as belonging to the unknown region T_U (trimap unknown) and the empty pixels as the foreground region T_F (trimap foreground) as empty (i.e., $T_F = \emptyset$).

1.2) Set $\alpha_n = 0$ for pixels $z_n \in T_B$ and $\alpha_n = 1$ for pixels $z_n \in T_U$ and initialize the foreground/background GMMs based on the pixels with label values of 1 and 0, respectively.

Step 2: Automatic iterative segmentation

2.1) Label each pixel z_n in T_U using the foreground/background GMMs and set k_n equal to the number of the Gaussian distribution with the highest weighted probability.

2.2) Update the GMM parameter θ based on the GMM labels of the pixels ($\theta = \text{argmin } U(a, k, \theta, z)$).

2.3) Construct an s-t network for T_U and segment the network using the maximum flow/minimum cut algorithm.

Step 3: Manual editing

3.1) For an image with relatively large segmentation errors, manually add or remove labels to update the pixels corresponding to T_B , T_U and T_F .

3.2) Repeat Step 2.3) to re-segment the image and thus

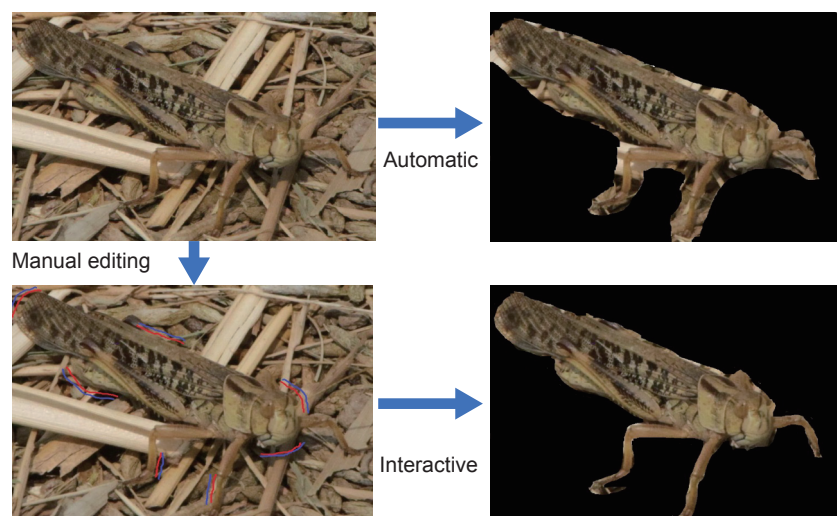


Fig. 2 Schematic diagram of locust image segmentation in a complex field environment.

obtain the corrected results.

Ultimately, we used the GrabCut segmentation method to segment all 1 200 locust images and extract four body parts (i.e., the head, hind legs, pronotum and wings) of the locusts. Thus, we obtained 4 800 images via segmentation, as shown in Fig. 3.

2.4. Method for extracting features from locust images

Based on analysis of the morphological features of the locust species considered here, it was preliminarily determined that *L. migratoria manilensis* and *O. decorus asiaticus* should be distinguished based on four parts of the body, namely, the wings, pronotum, hind legs and head. The locust instar can then be determined based on the morphology of the wings. A graph-theory-based segmentation method was used to extract segmented images of the head (top view and side view), pronotum, wings and hind legs of each locust. Additionally, three types of features, namely, textural, color

and morphological features, were extracted from the locust images, as shown in Table 2. The textural features are based on the results obtained by Ulaby *et al.* (1986). Based on the grayscale cooccurrence matrix proposed by Haralick *et al.* (1973), the Contrast, correlation, entropy, stationarity and second moment can be calculated as feature variables. The color features are based on the results obtained by Stricker and Markus (1995). The first moment coefficient μ_i (eq. (7)) and the second moment coefficient σ_i (eq. (8)) are selected to represent the color distribution features of an image (where p_{ij} is the grayscale value of pixel j in color channel i and n is the total number of pixels).

$$\mu_i = \frac{1}{N} \sum_{j=1}^N p_{ij} \quad (7)$$

$$\sigma_i = \left(\frac{1}{N} \sum_{j=1}^N (p_{ij} - \mu_i)^2 \right)^{\frac{1}{2}} \quad (8)$$

The morphological features consist of six variables, namely, the area, center of gravity, Euler's number, eccentricity, length of the major axis of the ellipse and speckle area ratio. All indicators are shown in Fig. 4, with

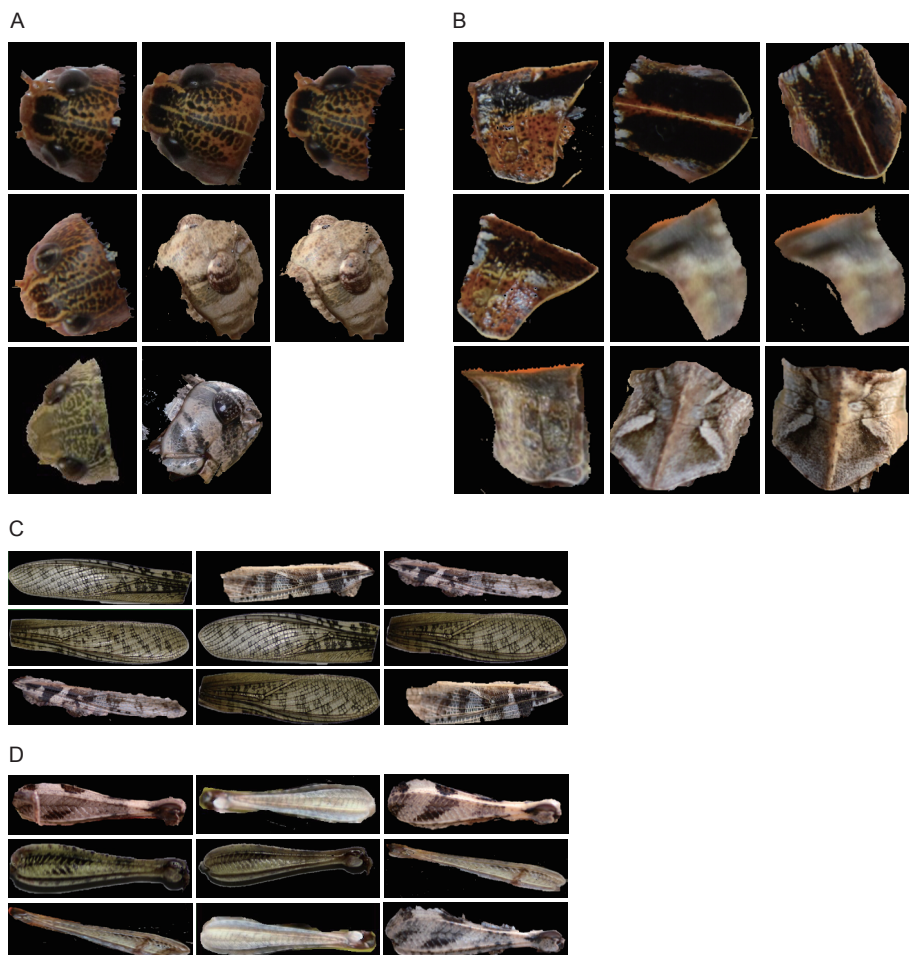


Fig. 3 Schematic diagram of the segmentation of various body parts in locust images. A, examples of locust head data. B, examples of locust pronotum data. C, examples of locust hind leg data. D, examples of locust wing data.

Table 2 Comparison of typical feature samples from *Locusta migratoria manilensis* and *Oedaleus decorus asiaticus*

Image features	Body part	<i>L. migratoria manilensis</i>		<i>O. decorus asiaticus</i>	
		Features	Example images	Features	Example images
Textural features	Wings	Forewings: black speckles		Forewings: large dark stripes; hind wings: dark crescent-shaped bands	
	Hind legs	Small black speckles		Large black speckles	
	Pronotum	Black bands on the side of the median carina		X-shaped stripes on the back	
Morphological features	Head	Round anterior margin		Elliptical	
Color features	Hind legs	Light yellow, occasionally with motes of light red		Yellowish-brown, light and dark red	

a total of 72 feature variables.

The preliminarily selected feature variables corresponding to the three types of features were initially screened by calculating the coefficients of variation (CV) and were then filtered via principal components analysis (PCA). The main steps are as follows:

Step 1: Calculate the mean value $\bar{\mu}$ and variance σ of each feature variable and remove any data outside the interval of $\bar{\mu} \pm 2\sigma$, which are treated as outliers.

Step 2: Calculate CV for each feature variable ($CV = (SD/\text{Mean})$, where SD is the standard deviation and Mean is the mean value) and remove any feature variables with $CV \geq 15\%$ (Fu et al. 2014).

Step 3: Use PCA to calculate the contributions of the remaining feature variables to identify the most important features.

2.5. SVM-based locust species and instar identification method

Via a nonlinear mapping, the SVM mode maps samples to a high-dimensional or even infinite-dimensional feature space, and thereby transforming a nonlinear separability problem in the original sample space into a linear separability problem in the feature space. For a sample set that cannot be linearly

processed in a low-dimensional space, once the samples are mapped to a suitable high-dimensional space (dimension raising), linear segmentation (or regression) can generally be achieved via a linear hyperplane in the high-dimensional space. However, dimension raising often complicates the computation process. The SVM method addresses the computational complexity caused by dimension raising by applying the kernel function expansion theorem. Because the SVM method involves the construction of a linear learning machine in a high-dimensional feature space, this method does not substantially increase the computational complexity compared to a linear model and, to some extent, avoid the “curse of dimensionality”. Common kernel functions include linear kernel functions, polynomial kernel functions, radial basis functions and two-layer neural network kernel functions.

2.6. Experimental process

The experimental process involved three stages, namely, data acquisition, model design and model testing, as shown in Fig. 5. In the data acquisition stage, we collected images of locusts of different species and instars in the field, performed image processing (including locust framing, species and instar information labeling, cropping, image

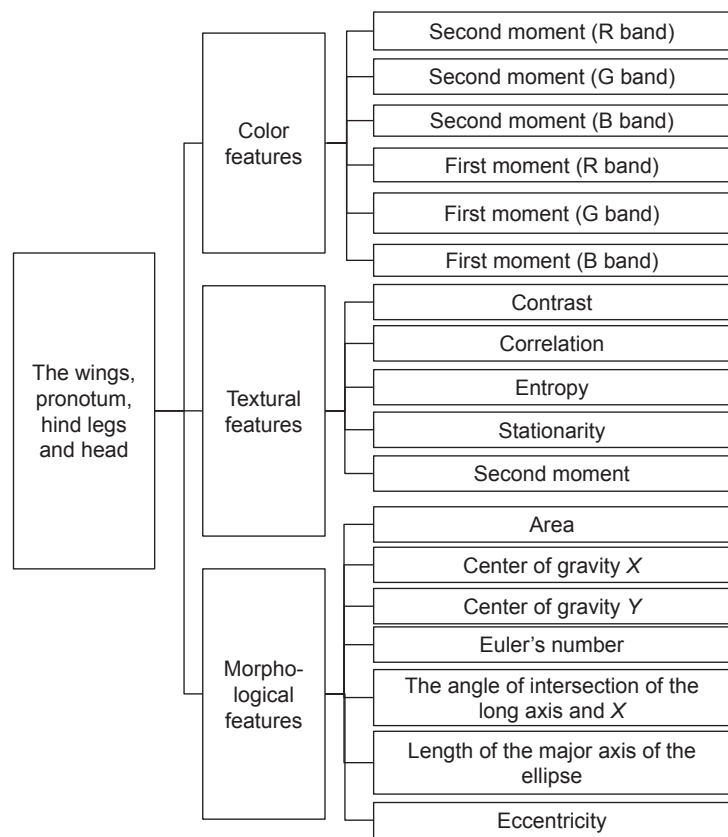


Fig. 4 The feature variables of in locust images. R band, red band; G band, green band; B band, blue band.

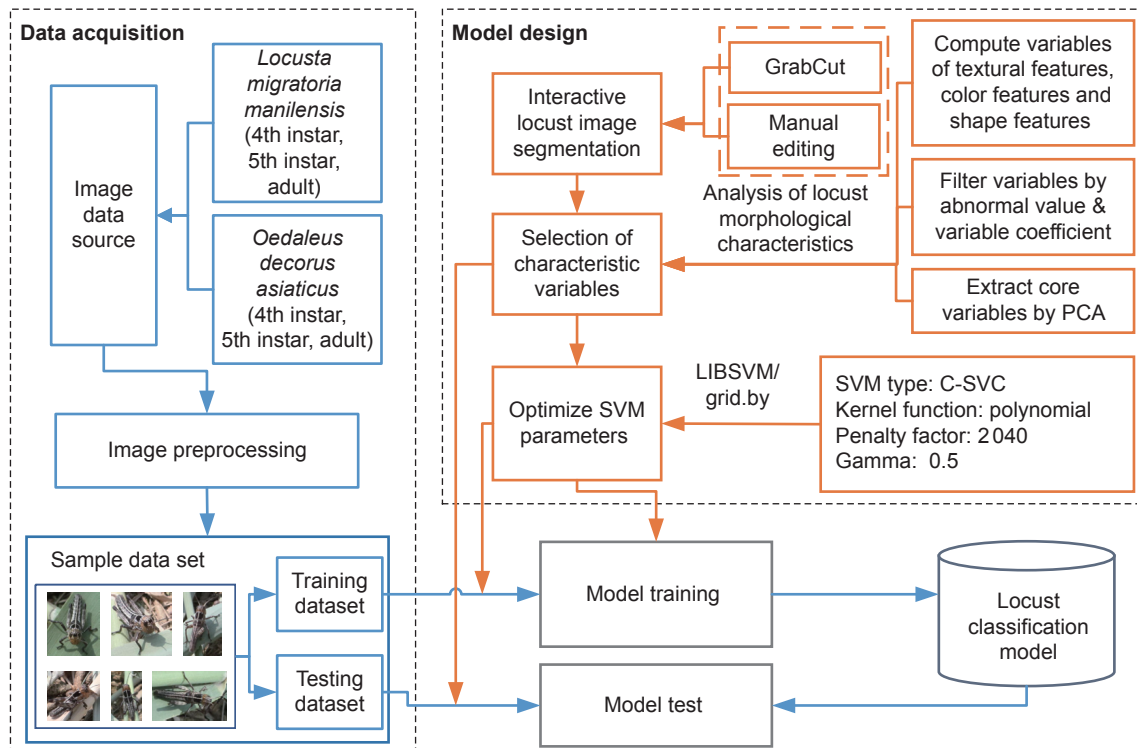


Fig. 5 Locust image classification test process. SVM, support vector machine; PCA, principal components analysis; C-SVC, C-support vector classification.

graying and histogram equalization enhancement (Luis et al. 2011; Li et al. 2014), and constructed a sample dataset for locust classification (total number of samples: 1 200). In the model design stage, based on an analysis of the morphological features of larvae of *L. migratoria manilensis* and *O. decorus asiaticus*, we designed a locust image segmentation method, extracted the feature variables of the locusts, selected the SVM model parameters, and developed a semi-automatic classification program. In the model testing stage, we input the feature variables extracted from the training samples, executed the model training process, constructed a locust classification model, and examined the accuracy of the model using the test dataset.

3. Results

3.1. Comparative analysis of different image segmentation algorithms

In order to achieve locust and background segmentation, commonly-used image segmentation algorithm experiments, including Otsu's threshold segmentation, iterative threshold segmentation, Robert edge segmentation, Sobel edge segmentation, LOG edge segmentation and GrabCut, had been done. From the results shown in Fig. 6, the GrabCut is the best segmentation algorithm in the case. In order to achieve fine segmentation, simple manual participation is required.

3.2. Extraction experiment of locust feature variable

As mentioned previously, we statistically calculated the

feature variables (as Fig. 4 shows) corresponding to the textural, color and morphological features of the various segmented body parts of the locusts in the training sample images and preliminarily screened the feature variables by identifying outliers and calculating CV. After this screening process, 18 feature variables remained out of a total of 73 initial feature variables.

Table 3 shows the mean difference of the feature variables corresponding to each body part between adults of *L. migratoria manilensis* and *O. decorus asiaticus*. It could be concluded that for the head part, homogeneity is the most significant variable, second moment (R band, G band and B band) are also outstanding; to the pronotum part, second moment (B band) is the most significant variable; spot area ratio and first moment (B band) are most significant variable respectively to hind leg and wing.

PCA has been used to calculate the contributions of the remaining feature variables to identify the most important features. As shown in Table 4, we ultimately selected the six principal components with the highest contributions, which together had a cumulative contribution level of 62.59%, corresponding to feature variables are the homogeneity and first moment (B band) of the head, the smoothness and first moment (B band) of the pronotum and the speckle area ratio of the hind leg.

3.3. Experiment of locust classification

Kernel function directly affects the accuracy of classification. Commonly-used kernel functions of SVM include linear, polynomial, radial basis function and sigmoid. To detect optimal kernel function, four kernel functions-based SVM

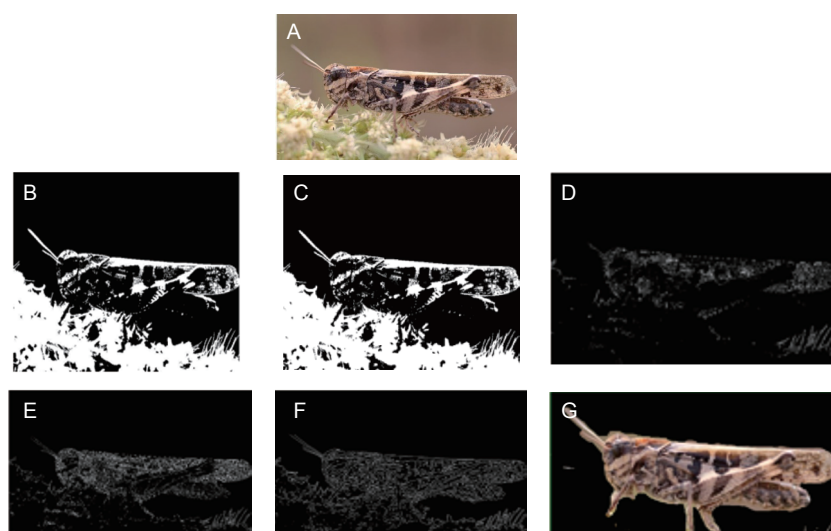


Fig. 6 Six kinds of image segmentation results. A, original image. B, Otsu's threshold segmentation. C, iterative threshold segmentation. D, Robert edge segmentation. E, Sobel edge segmentation. F, LOG edge segmentation. G, GrabCut.

models (SVM type: C-support vector classification) have been constructed and applied to identify locust species and instars. Additionally, tool in the LIBSVM library has been used to calculate the optimal values of the parameters c and g through grid search. The optimal values of c and g were determined to be 2 040 and 0.5, respectively. The classification accuracy has been listed in Table 5. Polynomial kernel function-based SVM model presents the highest overall recognition accuracy (79.34%).

However, by using PCA dimension reduction, classification efficiency has been improved, but the accuracy been reduced, recognition accuracy of locust with 4th or 5th instar is generally low. Hence in the following experiment, additional feature variables have been integrated to principal component variables to promote classification accuracy, as Table 6 shows. According to our comparison result, the

overall recognition accuracy can achieve 96.1% by using entropy of pronotum, wing area and wing length of the major axis of the ellipse as additional feature variable with PCA results. The recognition accuracy of 4th or 5th instar is also significantly improved.

4. Discussion

Image segmentation technology is the basis of machine learning. Selection of segmentation algorithm was mainly determined by the shape of the image to be segmented, the distribution characteristics of pixels, and whether there were specific regions or other factors that affect segmentation. Hence different segmentation algorithms present different segmentation effects. The segmentation algorithm in this paper can not only separate the image of locusts from the

Table 3 Variance analysis results of the feature variables between adults of *Locusta migratoria manilensis* and *Oedaleus decorus asiaticus*

Body part	Feature variable	Locust type		Body part	Feature variable	Locust type	
		<i>L. migratoria manilensis</i>	<i>O. decorus asiaticus</i>			<i>L. migratoria manilensis</i>	<i>O. decorus asiaticus</i>
Head	Homogeneity	2.83	3.71	Pronotum	Contrast	1.99	1.87
	Smoothness	0.47	0.51		Smoothness	0.46	0.47
	Entropy	0.01	0.04		Correlation	0.55	0.56
	Second moment (R band)	1.15	1.47		Second moment (B band)	0.90	1.89
	Second moment (G band)	1.05	1.42		First moment (B band)	1.19	0.16
	Second moment (B band)	0.97	1.34		Wing	Smoothness	0.49
	First moment (B band)	1.19	1.60		Correlation	0.54	0.48
Hind leg	Smoothness	0.51	0.51		First moment (B band)	1.15	0.55
	Correlation	0.58	0.57				1.67
	Spot area ratio	0.06	0.21				

Table 4 Principal component analysis (PCA) results for the locust feature variables

Principle component	Initial eigenvalues and contributions		
	Eigenvalue	Contribution (%)	Cumulative contribution (%)
1	30.73	21.64	21.64
2	16.28	11.46	33.11
3	13.53	9.53	42.64
4	11.36	8.00	50.64
5	9.59	6.75	57.40
6	7.37	5.19	62.59

Table 5 Performance comparison of support vector machine (SVM) with different kernel functions

Kernel function	<i>Locusta migratoria manilensis</i> recognition accuracy (%)			<i>Oedaleus decorus asiaticus</i> recognition accuracy (%)			Overall recognition accuracy (%)
	4th instar	5th instar	Adult	4th instar	5th instar	Adult	
Linear	56.42	67.11	73.23	55.63	60.67	73.79	64.47
Polynomial	78.28	76.32	91.39	71.41	69.50	89.14	79.34
Radial basis function	71.22	70.30	87.21	69.28	68.43	86.40	75.47
Sigmoid	67.21	78.33	84.23	69.42	73.22	80.31	75.45

Table 6 Performance comparison of support vector machine (SVM) with different feature variables

Feature variables	<i>Locusta migratoria manilensis</i> recognition accuracy (%)			<i>Oedaleus decorus asiaticus</i> recognition accuracy (%)			Overall recognition accuracy (%)
	4th	5th	Adult	4th	5th	Adult	
Principal component analysis (PCA)	78.32	76.31	91.41	71.41	69.53	89.07	79.34
PCA+Entropy pronotum	84.69	88.51	92.82	73.20	74.88	91.00	84.18
PCA+Entropy pronotum+Wing area	89.68	87.91	97.21	86.32	88.22	94.12	90.58
PCA+Entropy pronotum+Wing area+Wing length of the major axis of the ellipse	95.63	95.78	98.61	94.51	94.32	98.12	96.16

background, but also segment different body parts of locusts, which lay a foundation for future research. However, the segmentation algorithm is semi-automatic, which severely limits the efficiency and performability for realizing automatic locust monitoring in the field. CNN-based image semantic segmentation is developing rapidly and achieving automatic image segmentation (Li et al. 2019). However, there are still many challenges should be resolved for realizing fine segmentation of locust with different instars. For practical application, it is necessary to use comprehensive observation technologies (e.g., hyperspectral and laser point cloud technologies) and deep-learning-based image detection models to develop an automatic segmentation method to automatically extract sample image segments of various locust body parts in images acquired in complex field environments with various elements (e.g., plants, soil, rocks and various types of insects).

In this paper, a mature machine learning technology has been applied to implement identification of locust species and instars between *L. migratoria manilensis* and *O. decorus asiaticus*. By analyzing specific features of research objects, 73 characteristic variables have been extracted. And then outlier identification, variation analysis, PCA method and repeated SVM based classification tests have been used comprehensively to extract 8 variables as SVM model input. By using these variables, the efficiency of model trained has been improved, and the classification accuracy has been enhanced. An SVM-based classification model of locust is constructed in this paper, and the recognition accuracy of this model can achieve 96.16%. The comparison result shows that the extracted locust characteristic variables are effective. It gives us an inspiration to combine our classification process with deep learning technology to improve disadvantage of deep learning technology, such as massive samples requirement, poor model generalization.

In the field, even for locusts with the same species and instars, the occlusion, posture and body color may be different as the living environment changes, which limit the generalization of the deep learning model. The 8 variables in this paper are key variables to distinguish species and instars of locust. The CNN-based classification model can be improved and applied in identification of locust species

and instars by integrating with histogram of oriented gradient feature graphs of above 8 variables.

Furthermore, several problems must be addressed before applying the proposed model for the semi-automatic acquisition of quadrat-scale locust instar, species and observation data of distribution density in practice. First, this study considered feature variables extracted from RGB images alone, which cannot represent the differences in the reflectance of an observation target in different spectral bands. In subsequent studies, it will be necessary to use hyperspectral images to optimize the selection of the feature variables for locust image classification. Moreover, this study demonstrated semi-automatic detection only for *L. migratoria manilensis* and *O. decorus asiaticus* (including locusts of the 4th instar, 5th instar and adult stages) as examples. In subsequent studies, it will be necessary to further expand the locust species and instar sample database to enhance the capacity for automatic locust information acquisition. Our future work will focus on the development of a field device for automatically acquiring and transmitting locust species, instar and distribution density information. We will study how the locust distribution density and structural changes in locust communities are related to the hydrothermal and vegetation growth conditions in their habitats in various regions based on large amounts of quadrat-scale observation data (Ye et al. 2016, 2017, 2018) and investigate how to realize integrated applications using both quadrat-scale locust observation data and multisource satellite remote sensing data.

5. Conclusion

This study has proposed a semi-automatic locust species and instar information detection model based on locust image segmentation, locust feature variable extraction and SVM-based classification. The locust image segmentation experiment showed that the proposed GrabCut-based interactive segmentation method can be used to rapidly extract sample images of various locust body parts (i.e., the head, pronotum, wings and hind legs) with high operability. The SVM-based locust classification experiment showed an automatic detection accuracy of 96.16% by using a

polynomial kernel function with a c value of 2040 and a g value of 0.5. In summary, the proposed detection model exhibits high performance and accuracy when used to identify locust instars of the species *L. migratoria manilensis* and *O. decorus asiaticus*.

Acknowledgements

This research was funded by the National Natural Science Foundation of China (31471762) and the Fundamental Research Funds for the Central Universities of China (2018NTST03). We would like to thank the Center for Geodata and Analysis, Faculty of Geographical Science, Beijing Normal University, China for providing high-performance computing support.

References

- Bryceson K P, Wright D. 1986. An analysis of the 1984 locust plague in Australia using multitemporal landsat multispectral data and a simulation-model of locust development. *Agriculture Ecosystems & Environment*, **16**, 87–102.
- Cai Q, He D J. 2010. Identification of vegetable leaf-eating pests based on image analysis. *Journal of Computer Applications*, **30**, 1870–1872. (in Chinese)
- Chen T, Zeng J, Xie C, Wang R, Liu W, Zhang J, Li R, Chen H, Hu H, Dong W. 2019. Intelligent identification system of disease and insect pests based on deep learning. *China Plant Protection*, **39**, 26–34. (in Chinese)
- Deng L M, Wang Y J, Han Z Z, Yu R S. 2018. Research on insect pest image detection and recognition based on bio-inspired methods. *Biosystems Engineering*, **169**, 139–148.
- Din Y Q, Li D M, Chen Y P. 1978. Studies on the patterns of distribution of the oriental migratory locust and its practical significance. *Acta Entomologica Sinica*, **21**, 243–259. (in Chinese)
- Fu N, Liu X G, Zhang Q, Zhang Y, Yang Q. 2014. Variation pattern of rice irrigation water requirement in Southwest of China. *Chinese Journal of Ecology*, **33**, 1895–1901. (in Chinese)
- Gómez D, Salvador P, Sanz J, Casanova C, Taratiel D, Casanova J L. 2019. Desert locust detection using Earth observation satellite data in Mauritania. *Journal of Arid Environments*, **164**, 29–37.
- Guo Z Y, Shi W P, Zhang L. 2004. Behavioral and morphological indices for phase transformation of oriental migratory locust *Locusta migratoria*. *Chinese Journal of Applied Ecology*, **15**, 859–862. (in Chinese)
- Haralick R, Shanmugam K, Dinstein I. 1973. Textural features for image classification. *IEEE Transactions on Systems, Man, and Cybernetics (Systems)*, **3**, 610–621.
- Li H, Cai Y, Wang L. 2019. Image semantic segmentation based convoluted network with global feature extraction. *Infrared Technology*, **41**, 595–615.
- Li L, Zhu D, Ye S J, Yao X, Zhang N. 2014. Design and implementation of geographic information systems remote sensing and global positioning system-based information platform for locust control. *Journal of Applied Remote Sensing*, **8**, 89–99.
- Lu H, Yu M, Zhang L S, Zhang Z, Long R. 2006. Effects of foraging by different instar and density of *Oedaleus asiaticus* B Bienko on forage yield. *Plant Protection*, **31**, 55–58. (in Chinese)
- Luis O, Rodrigo C, Juan J. 2011. Scale invariant feature approach for insect monitoring. *Computers and Electronics in Agriculture*, **75**, 92–99.
- Ren B Y, Yang P Y, Zhu J Q, Wei Q W. 2017. The effect and prospect of locust disaster sustainable control in China. *China Plant Protection*, **37**, 55–57. (in Chinese)
- Solis-Sánchez L O, Castañeda-Miranda R, García-Escalante, J, Pacheco I. 2011. Scale invariant feature approach for insect monitoring. *Computers and Electronics in Agriculture*, **75**, 92–99.
- Stricker M A, Markus O. 1995. Similarity of color images. *The International Society for Optical Engineering*, **2420**, 381–392.
- Thenmozhi K, Srinivasulu R. 2019. Crop pest classification based on deep convolutional neural network and transfer learning. *Computers and Electronics in Agriculture*, **164**, 104906–1049016.
- Ulaby F T, Kouyaté F, Brisco B, Williams T. 1986. Textural information in SAR Images. *IEEE Transactions on Geoscience and Remote Sensing*, **24**, 235–241.
- Wang J N, Chen X L, Hou X W, Zhou L, Zhu C, Ji L. 2017. Construction, implementation and testing of an image identification system using computer vision methods for fruit flies with economic importance (Diptera: Tephritidae). *Pest Management Science*, **73**, 1511–1528.
- Wang X, Fang X, Yang P, Jiang X, Jiang F, Zhao D, Li B, Cui F, Wei J, Ma C. 2014. The locust genome provides insight into swarm formation and long-distance flight. *Nature Communications*, **5**, 2957.
- Wen G H, Bai Y, Zhou J. 2015. Geometric morphometric analysis of wing shape variation in five *Oxya* spp. grasshoppers. *Chinese Journal of Applied Entomology*, **52**, 356–362. (in Chinese)
- Van der Werf W, Woldewahid G, Van Huis A, Butrous M, Sykora K. 2005. Plant communities predict the distribution of solitarious desert locust *Schistocerca gregaria*. *Journal of Applied Ecology*, **42**, 989–997.
- Xie C, Wang, R, Zhang J, Chen P, Dong W, Li R, Chen T, Chen H. 2018. Multi-level learning features for automatic classification of field crop pests. *Computers and Electronics in Agriculture*, **152**, 233–241.
- Xie C, Zhang J, Li R, Li J, Hong P, Xia J, Chen P. 2015. Automatic classification for field crop insects via multiple-task sparse representation and multiple-kernel learning. *Computers and Electronics in Agriculture*, **119**, 123–132.
- Xiong X M, Wang Y, Zhang X. 2007. Detection of locusts using near-infrared spectroscopy and cluster analysis. In: *Actual*

- Tasks on Agricultural Engineering International Symposium on Agricultural Engineering.* Opatija, Croatia.
- Yao Q, Chen G, Wang Z, Zhang C, Yang, B, Tang J. 2017. Automated detection and identification of white-backed planthoppers in paddy fields using image processing. *Journal of Integrative Agriculture*, **16**, 1547–1557.
- Ye S J, Liu D, Yao X, Tang H, Xiong Q, Zhuo W, Huang J, Zhu D, Cheng C, Song C. 2018. RDCRMG, a raster dataset clean & reconstitution multi-grid architecture for remote sensing monitoring of vegetation dryness. *Remote Sensing*, **10**, 1376.
- Ye S J, Yan T L, Yue Y, Lin W, Li L, Yao X, Mu Q, Li Y, Zhu D. 2016. Developing a reversible rapid coordinate transformation model for the cylindrical projection. *Computers & Geosciences*, **89**, 44–56.
- Ye S J, Zhang C, Wang Y, Liu D, Du Z, Zhu D. 2017. Design and implementation of automatic orthorectification system based on GF-1 big data. *Transactions of the Chinese Society of Agricultural Engineering*, **33**, 266–273. (in Chinese)
- Ye S J, Zhu D H, Yao X C, Zhang N, Fang S, Li L. 2014. Development of a highly flexible mobile GIS-based system for collecting arable land quality data. *IEEE Journal of Selected Topics in Applied Earth Observations and Remote Sensing*, **5**, 4432–4441.
- Zhang J. 2013. Research and application of diagnosis technologies for crop pests based on image recognition. Ph D thesis, University of Science and Technology of China, China. (in Chinese)
- Zhang Y D, Wu L N, Wei G, Wu H Q. 2009. Improved split-merge segmentation used for locust image. *Computer Engineering and Applications*, **14**, 34–38.
- Zhen Y J, Wu G, Wang Y M, Mao W H. 2010. Locust images detection based on fuzzy pattern recognition. *Transactions of the Chinese Society of Agricultural Engineering*, **26**, 21–25. (in Chinese)

Executive Editor-in-Chief WAN Fang-hao
Managing editor SUN Lu-juan